Heliyon

Received:
5 November 2018
Revised:
1 January 2019
Accepted:
1 March 2019

Cite as: Dana C. Bernhardt, Nora M. A. Ponce, Maria F. Basanta, Carlos A. Stortz, Ana M. Rojas. Husks of *Zea mays* as a potential source of biopolymers for food additives and materials' development. Heliyon 5 (2019) e01313. doi: 10.1016/j.heliyon.2019.e01313

Husks of *Zea mays* as a potential source of biopolymers for food additives and materials' development

Dana C. Bernhardt [a,c], **Nora M. A. Ponce** [b,c], **Maria F. Basanta** [a,c], **Carlos A. Stortz** [b,c], **Ana M. Rojas** [a,c,*]

[a] *Departamento de Industrias-ITAPROQ, Argentina*

[b] *Departamento de Química Orgánica-CIHIDECAR, Facultad de Ciencias Exactas y Naturales, Universidad de Buenos Aires, Ciudad Universitaria, C1428BGA Buenos Aires, Argentina*

[c] *CONICET, Argentina*

[*] Corresponding author.
E-mail address: arojas@di.fcen.uba.ar (A.M. Rojas).

Abstract

Maize husks, an agricultural and industrial residue generated in a large volume, were investigated as a potential source of useful biopolymers. Thus, their chemical composition was firstly studied, after which two biopolymer products were obtained and characterized. Maize husks were dried and milled, obtaining a 210 μm-main particle size powder (MHP). It contained carotenes (4 mg/100 g), and exhibited antioxidant capacity (≈195 mg ascorbic acid/100 g MHP) coming also from extractable coumaric and cinnamic acids-derivatives (14 mg/100 g). A 31% of the MPH was water-soluble at room temperature, mainly constituted by fructose, glucose, and sorbitol of mesophylls' intracellular origin. The water insoluble fiber (WIF, ≈70%), which showed antioxidant capacity (≈25−33 mg ascorbic acid/100 g WIF), was almost entirely constituted by the cell wall biopolymers or alcohol insoluble residue (AIR) of the MPH, mostly arabinoxylans (≈26%) crosslinked by ferulic residues (18.6 mg/100 g MPH), and cellulose (26%). Low levels of pectins (5.5%) and lignin (7%) were found. Hence, a 1.25%-sulfur nanocellulose (NCC) was directly obtained with sulfuric

https://doi.org/10.1016/j.heliyon.2019.e01313

acid (−15 mV Zeta-potential; 147 °C onset of thermal-degradation) without the necessity of previous delignification. On the other hand, a water soluble arabinoxylan enriched fraction (AX-EF) with pseudoplastic behavior in water and sensibility to calcium ions (≈3 Pa•s initial Newtonian-viscosity) was isolated by alkaline hydrolysis of diferulate bridges. Despite a 56% of crystallinity, NCC showed the highest water absorption capacity when compared to that of the AX-EF and AIR. Maize husks constitute an important source of biopolymers for development of materials and food additives/ingredients with relevant hydration and antioxidant properties.

Keyword: Food science

1. Introduction

Maize (*Zea mays* L.; Poaceae family) is an angiosperm, monocot plant of enormous modern-day economic importance as foodstuff and alternative energy source [1]. The maize stover is produced as a by-product after the maize grain is harvested [2], and it has been estimated at 75 million tons per year, with much more supply in the future [3]. This residue consists of stalk, leaf, cob and husk tissues that remain in the field and decompose, contributing to soil organic matter [2]. In the 2017/2018 campaign, 35 million tons of maize was the estimated value to be harvested in Argentina, of which 18−33% are composed by husks and leaves [4]. The maize stover residue poses both disposal and environmental pollution problems, which result in the loss of nutritionally valuable materials. Processing of this material could yield valuable products [5].

As the cob and silk, the maize husks also constitute a major residue in the maize commercialization in markets for home consumption as well as in the industrialization. Vegetable waste processing and its elimination represent important costs for industries, often inaccurately evaluated. At the same time, there is a growing recognition in Europe that the twin problems of waste management and resource depletion can be solved together through the utilization of food wastes, which are now intended as an alternative carbon source to produce commercially viable chemical commodities [6]. These by-products can add high value to the raw materials while they contribute to a sustainable development and environmental protection. Maize husks can constitute other cellulose-rich agricultural residue. Nanomaterials could be produced from the biopolymers obtained from agricultural residues such as rice straw, maize and coconut husks that are locally available in several countries for possible applications as reinforcing filler material in bioplastics [7, 8]. Also, maize husk is investigated for paper production. Since it contains fibrillar cellulose, it stands to be a potential source for pulp with lower environmental degradation threats than wood [9]. Fiber-rich by-products such as maize husk can be also applied

https://doi.org/10.1016/j.heliyon.2019.e01313

as a source of functional food additives and ingredients [10, 11] and of dietary fiber [12]. They can be incorporated into food products as inexpensive, low-caloric bulking agents for partial replacement of flour, fat or sugar, as enhancers of water and oil retention and to improve emulsion or oxidative stabilities [13]. Also, functional oligosaccharides may be enzymatically obtained from maize husks.

In order to determine the potential of maize husks to constitute an alternative carbon source for production of biopolymers and natural antioxidants, it is first necessary to analyze the chemical composition, mainly in relation to the substances of interest, as we attempt to perform in the present work. From this knowledge, alkaline and acid hydrolyses were separately performed to isolate, as two fiber enriched fractions, the main cell wall biopolymers. In view of their utility as food additives/ingredients and/or materials, the rheological performance and hydration properties were then evaluated in addition to their respective characterization.

2. Materials and methods

2.1. Chemicals

Deionized water from Milli-Q™ (USA) was used. Chemicals were of analytical quality. β-carotene, D-galacturonic acid, D-glucose, bovine serum albumin protein standard, α-amyloglucosidase (S9144), glucose-oxidase/peroxidase (G3660), *o*-dianisidine dihydrochloride, corn starch standard (S5296), chlorogenic acid, *p*-coumaric acid, and ferulic acid were from Sigma-Aldrich (Saint Louis, USA), and the rest of the chemicals were from Merck (Argentina). Glycemic kit was from Wiener Lab™ (Rosario, Argentina).

2.2. Sample preparation

Maize (*Zea mays* L.) husks discarded at markets and food industries were collected. They were the green, light green and slightly yellow colored outer shells. Husks were dried at 65 °C for 4 h under high air convection in order to obtain completely dried husks, which showed a brittle texture. Dried husks were transversally cut into strips of ≈15 mm-width and then milled through a cutting mill (Heavy-Duty Cutting Mill SM 300, Retsch, Germany) provided with a 500 μm mesh sieve. This "**maize husk powder**" (**MHP**) was separated by particle size. Weighed amounts were sieved through a vibratory sieve shaker (Retsch, Germany) provided with 840, 420, 210, 105, 53, 25 μm ASTM mesh sizes. Each fraction recovered between the two closest sieves was weighed for yield calculation and stored in hermetically sealed pouches.

A weighed (20 g) maize husk powder sample (210 μm) was submitted to extraction with deionized water (1:100 w/v) at room temperature (23 °C) for 24 h under

https://doi.org/10.1016/j.heliyon.2019.e01313

magnetic stirring, filtrated through a glass filter membrane (Whatman GF/C, UK) and washed with water. The solid residue was frozen and freeze-dried (**water insoluble fiber**"; **WIF**). The maize husk powder fraction dissolved by water had to be frozen with liquid nitrogen to avoid matrix collapse during freeze-drying. Yield was calculated with respect to MPH and chemical composition of the **WIF** was then determined. Reducing carbohydrates were quantified by the Somogyi-Nelson's spectrophotometric method [14], total carbohydrates (including polysaccharides) were determined through the phenol-sulfuric acid spectrophotometric method of Dubois et al. [15], measuring the absorbance at 485 nm, and using D-galacturonic acid and D-glucose for the standard curves. Uronic acids (UA) were determined through the spectrophotometric method of Filisetti-Cozzi and Carpita [16], adding sulfamic acid-potassium sulfamate to the samples before heating with a sulfuric acid-tetraborate mixture, to suppress the interfering browning of neutral monosaccharides that are simultaneously liberated. Proteins were determined according to the spectrophotometric assay of Lowry et al. [17] using bovine serum albumin as standard. In this procedure, under alkaline conditions, copper complexes with protein. According to Mattoo et al. [18], Lowry's assay, though multistepped is the method of choice for vegetable tissues. Fructose was determined through the HCl-resorcinol method [19], glucose by enzyme-specific glucose oxidation with glucose-oxidase followed by the phenol-4-aminophenazone colorimetric reaction (glycemic kit) [20]. The identity of polyols and sugars was determined through gas chromatography with previous sample hydrolysis with CF_3COOH (2M TFA, 90 min at 120 °C), reduction with $NaBH_4$ and conversion to alditol acetates, as explained by Basanta et al. [21], eventually with the aid of a gas chromatograph (GC) linked to a mass spectrometric detector (GC/MS), after treatment of part of a freeze-dried sample with 3.5 volumes of isopropanol for precipitation. The soluble fraction was dried in a rotary evaporator (Büchi, Germany), and analyzed for the presence of sugars and polyols.

On the other hand, a weighed (20 g) WIF sample was submitted to cell wall biopolymer extraction with boiling 85% v/v ethanol (70 mL) for 30 min under stirring into a lab hood. The suspension was filtered (Whatman GF/C, UK) and the residue was washed three times with boiling 95%-ethanol. The last residue retained by the membrane was left under the lab hood for ethanol evaporation, then frozen and freeze-dried, constituting the "**alcohol insoluble residue**" (**AIR**).

2.2.1. Alkaline hydrolysis of the AIR

The AIR (30.00 g) was dispersed in 1000 mL of an aqueous solution of KOH 4% w/v and stirred for 24 h at 25 °C. Afterwards, the dispersion was filtrated under vacuum through a glass filter membrane (Whatman GF/C, UK), and the residue was washed in the filter with deionized water. The filtrate was then neutralized with HCl (37% w/w), after which 2 volumes of ethanol 96% v/v were added. The system was left

https://doi.org/10.1016/j.heliyon.2019.e01313

overnight at 5 °C for complete insolubilization of the polysaccharides dissolved in the KOH 4%. The precipitate was separated by filtration through a glass filter membrane (Whatman GF/C, UK), and washed three times with 96% v/v-ethanol. It was then left under convection into the lab hood for drying. The dried powder (**AX-EF**) was weighed to calculate the yield with respect to the AIR, and finally milled (IKA A10 Basic, Germany). The AX-EF was produced in triplicate.

2.2.2. Acid hydrolysis of the AIR

The AIR (2 g accurately weighed) was dispersed under stirring in 25 mL of deionized water for 10 min, after which the system was immersed into an ice bath maintaining a vigorous and constant agitation while 30 mL of concentrated (98.0% w/w) sulfuric acid solution were added drop to drop from a burette to avoid carbonization [22, 23]. A 64% w/w sulfuric acid solution was finally obtained in the AIR dispersion. After 2 h of stirring at 45 °C, 100 mL of deionized water were added to stop the reaction. The system was centrifuged at 10,000 rpm for 10 min at 6.0 °C (Eppendorf 5804R, Germany), the pellet was then separated from the supernatant and washed by re-dispersion in deionized water followed by centrifugation as above described. The latter procedure was repeated four times. The final washed residue suspended in deionized water was then dialyzed for three days at 4 °C through a 10,000−12,000 Da molecular weight cutoff membrane. Finally, the content of the dialysis bag was sonicated for 30 min at room temperature, then frozen and freeze-dried (Christ Alpha 1−4 LD; Pfeiffer pump Duo 5M, Germany). The dried powder obtained was considered a fraction enriched in crystalline cellulose (**NCC**), which was weighted to calculate the yield with respect to the AIR. The NCC was produced in triplicate.

2.3. Chemical analyses

Carotenes were determined in MPH, WIF and AIR (0.2500 g) according to Biswas et al. [24], using β-carotene as standard. Total starch was determined in the AIR through the enzymatic method involving α-amylase, amyloglucosidase and *o*-dianisidine of Karkalas [25]. As above, proteins were also determined in the AIR and AX-EF (≈0.0100 g) through the assay of Lowry et al. [17]. In the AX-EF, total polysaccharides and UA were also respectively determined through the phenol-sulfuric acid method [15], and the spectrophotometric assay of Filisetti-Cozzi and Carpita [16].

Cellulose, lignin, non-cellulosic polysaccharides (pectins and hemicelluloses) and UA of pectins were separately determined by selective extraction from 0.0100 g of the AIR with different concentrations of sulfuric acid (1 M or 72% w/w), as reported by Ng et al. [26] and Basanta et al. [12]. Cellulose and lignin were separately quantified by weighing the respective insoluble residues obtained after extraction with either 1M-sulfuric acid aqueous solution, which dissolves only the non-

https://doi.org/10.1016/j.heliyon.2019.e01313

cellulosic polysaccharides (pectins and hemicelluloses), or 72% w/w sulfuric acid, which dissolves cellulose but not lignin. In the supernatants of the 1M sulfuric acid treatments, total or non-cellulosic polysaccharides were determined, as above explained, by the phenol-sulfuric acid method [15], and UA by the technique of Filisetti-Cozzi and Carpita [16].

2.3.1. Sequential extraction of cell wall polymers (AIR) and chemical analyses

Cell wall polymer fractionation was performed through the sequential extraction of the AIR (Fig. 1), as reported by Basanta et al. [21]. Briefly, 12 g of AIR was subsequently stirred for 24 h with 0.05 M CDTA (pH 6.0), 0.1 M Na_2CO_3, 4% KOH and 24% KOH, which produced the fractions soluble in CDTA (CSF), Na_2CO_3 (NSF) and 4% and 24% KOH (4KSF and 24KSF, respectively) (Fig. 1). Extracts and

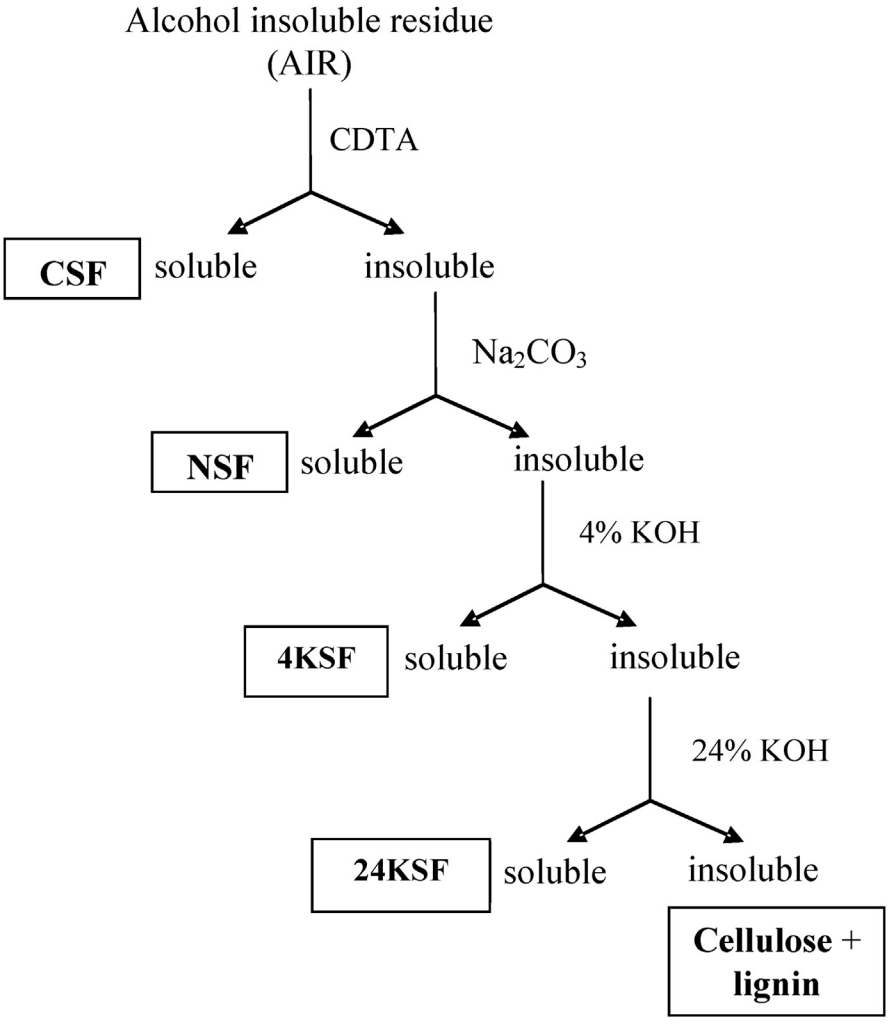

Fig. 1. Sequential extraction of the cell wall polymers performed on the AIR of maize husks.

https://doi.org/10.1016/j.heliyon.2019.e01313

residues obtained were freeze-dried after washing and dialyzing. Determinations of UA, total polysaccharides and protein content, as well as determination of the neutral sugar (NS) composition [21] were performed in triplicate on each sample.

To determine the NS composition, hydrolysis of the cell wall polysaccharides was carried out with 2 M TFA (90 min; 120 °C). Hydrolyzates were derivatized to the alditol or aldononitrile acetates and analyzed by gas chromatography (GC) using a capillary column (30 m × 0.25 mm) coated with SP-2330 (0.20 μm) on a HP-5890 Gas Chromatograph equipped with a flame ionization detector (FID). Nitrogen was used as the carrier gas, with a flow rate of 1 mL/min and a split ratio of 90:1. Chromatography runs were isothermal at 220 °C, while the injector and detector were set at 240 °C. Myo-inositol was used as internal standard for the alditol acetates, and D-lyxose for the aldononitrile acetates. When a confirmation of identity was needed, the GC-MS analyses were carried out on a Shimadzu QP 5050 A GC/MS apparatus working at 70 eV using similar conditions to those described above, but using He as gas carrier with a split ratio of 60:1.

2.3.2. Analysis of phenolic compounds in MPH

Non-bound or extractable phenolics were isolated from approximately 2.5 g of MPH through the acetone/water/acetic acid (70:29.5:0.5 v/v/v) solvent followed by solid phase extraction (Sep-Pack C18 cartridges, Waters, USA), and analyzed by reversed-Phase HPLC-DAD (Waters 1525, Milford, MA, USA) and HPLC-ESI-MS-MS (Thermo Fisher Scientific Inc., San Jose, CA, USA), using a C18 column (250 × 4.0 mm, 5 μm particle size; Luna, Phenomenex, CA, USA), as explained by Basanta et al. [27].

Covalently attached phenolic compounds were isolated through alkaline hydrolysis (1 g MPH:15 mL 2 M NaOH) by stirring under vacuum in darkness, at 4 °C for 2 h, according to Vaidyanathan and Bunzel [28]. Afterwards, the pH was adjusted to 1.5 by addition of 6 M HCl. Three successive extractions with 25 mL of ethyl acetate were performed, the supernatants were combined and the solvent was evaporated at low pressure (Büchi rotavap, Germany). The residue was dissolved by addition of 1000 microliters of methanol, filtrated through 0.45 μm membrane, and analyzed by reversed-Phase HPLC-DAD and HPLC-ESI-MS/MS, as above indicated [27]. The mobile phase was constituted by the gradient between an aqueous solution of formic acid (1% v/v) and pure methanol. For the extractable phenolics, the HPLC was performed at a flow of 0.8 mL/min under a linear gradient of mobile phase that increased for 70 min from 10% to 66% of methanol. For the esterified phenolics, the HPLC was carried out at a flow of 0.5 mL/min with a linear gradient that increased linearly for 90 min from 10% to 82% of methanol. The UV spectra were recorded in the 200−800 nm wavelength range. Quantification was performed by the external standards' method. For the extractable phenolics, cinnamic acid

https://doi.org/10.1016/j.heliyon.2019.e01313

derivatives were quantified as chlorogenic acid at 320 nm, while the coumaric acid derivatives were quantified as *p*-coumaric acid at 310 nm. Covalently bound phenolics were quantified using ferulic acid as external standard, at 320 nm. Results were expressed as mg of the phenolic compound per 100 g of MPH.

Isolations were performed in triplicate ($n = 3$) from MPH for each kind of phenolics (non-bound and covalently bound compounds).

2.3.3. Elemental analysis of NCC through TXRF

The total reflection X-ray fluorescence (TXRF) technique was used to perform the elemental analysis of the NCC samples by using an S2 Picofox (Bruker, Germany) TXRF spectrometer provided with an air-cooled X-ray tube of 50 W for excitation, with Mo target, an SDD detector, a Peltier-cooled XFlash Silicon Drift Detector, an active area of 30/60 mm^2, and an energy resolution $<$149 eV. Determinations were performed in triplicate from each of the three batches of NCC produced.

2.4. Antioxidant capacity

It was determined through the radical scavenging activity of samples by using the DPPH (2,2-diphenyl-1-picrylhydrazyl) assay [29], and through the ferric reducing antioxidant power (FRAP) assay [30]. Three samples of each fiber fraction analyzed (MPH, WIF, AIR) were extracted with methanol and all results were expressed as L-(+)-ascorbic acid standard, using a standard dissolved in methanol.

2.5. Water activity

Water activity (a_W) of the isolated fibers was evaluated in triplicate (25.0 °C) through a Decagon AquaLab (Series 3 Water activity meter, USA), according to Basanta et al. [12].

2.6. Moisture

It was determined by drying at 70 °C under vacuum until constant weight ($\approx$22 d) into an oven (Gallenkamp, UK). Moisture was expressed as percentage on dry basis, which permitted to calculate the chemical composition results on dry basis. Determinations were carried out at least in triplicate.

2.7. Color

Fiber color was measured with a colorimeter (Minolta CM-508d, Japan) provided with a 1.5 cm-diameter aperture in the CIE*Lab* color space (D65 illuminant, 2° standard observer), as reported by Basanta et al. [12]. The average and standard deviation ($n > 6$) was reported.

https://doi.org/10.1016/j.heliyon.2019.e01313

2.8. Kinetics of spontaneous water absorption

Water absorption kinetics was evaluated in triplicate for the AIR, AX-EF and NCC through measurement of the spontaneous water uptake at 25 °C by an accurately weighed sample (0.0200−0.0400 g), as explained by Basanta et al. [21]. The experimental data of q (water absorbed at time t), in mL/g, was fitted by one of the following equations, which corresponded to the Ritger & Peppas' power law model shown in Eq. (1) [12] or the Boquet's model of Eq. (2) [21]:

$$q(t) = k \cdot t^n \tag{1}$$

$$q(t) = \frac{WBC \cdot t}{B + t} \tag{2}$$

where k and n are, respectively, the kinetic rate constant and the swelling exponent, while WBC is the maximal water absorption capacity or water binding capacity, and B is the time needed to absorb a half of the maximal water absorption (WBC/2).

2.9. Thermal gravimetric analysis (TGA)

Thermal decomposition of fibers was analyzed through a simultaneous thermal analyzer (TG-DSC/DTA TA Instruments SDT Q600, USA) equipped with a nitrogen flow device and a data acquisition system. Each sample ($\approx$ 10 mg), placed in an alumina pan, was thermally treated at 10 °C/min heating rate under N_2 (100 mL/min) from ambient temperature to 600 °C. The mass loss and calorific changes as a function of temperatures were recorded and used to plot the TG and derivative thermogravimetric (DTG) curves. Experiments were performed in triplicate.

2.10. X-ray diffraction

Samples were submitted to X-ray radiation through a Philips diffractometer (PW 1510, Netherlands) provided with a vertical goniometer operating at Cu K α radiation $\lambda = 1.542$ Å, 40 kV and 30 mA. X-ray intensity was recorded with a scintillation counter in a scattering angle (2θ) range of 6−33° (1°/min). Distances between the planes of the crystals d (Å) were calculated from the diffraction angles (°) obtained in the X-ray pattern, according to Bragg's law:

$$n\lambda = 2d \cdot \sin(\theta) \tag{3}$$

wherein λ is the wavelength of the X-ray beam and n is the reflection order, considered as 1 for calculation. The degree of crystallinity was calculated according to Xiao et al. [31].

https://doi.org/10.1016/j.heliyon.2019.e01313

2.11. Zeta potential

The *Z*p of the NCC samples was determined according to Carneiro-da-Cunha et al. [32] by using a Zetasizer Nano ZS (Malvern Instruments Limited, UK), provided with a 632.8 nm 'red' laser of 4 mW He-Ne gas, and a detection angle of 175°. A sample of 0.0010 g of NCC was dispersed in filtered deionized water by vortexing (pH 5.0). At room temperature, ten measurements were made per sample, and samples were evaluated in triplicate. It is reported the mean and standard deviation.

2.12. Viscosity

A sample of 0.1000 g of each suitable fiber fraction (AX-EF or 4KSF) was dissolved in enough amount of deionized water to obtain a 2.00% (w/w) solution, with vortexing and heating in a water bath at 70 °C for some seconds. Two solutions were prepared for each fiber fraction. They were then stored at 25 °C for 18 h in order to attain swelling equilibrium. Afterwards, calcium chloride (30 mg Ca^{2+}/g UA) was added under heating (water bath, 70 °C) to one of the two solutions of each fiber fraction (AX-EF or 4KSF). Flow curves were then recorded at steady-state in triplicate from samples of each fiber fraction solution studied, at 20.0 °C with a rheometer (Paar Physica MCR300, Austria) in the 0.001−200 rad•s^{-1} shear rate ($\dot{\gamma}$) range for 50 min. Serrated parallel plate geometry of 25 mm-diameter was used, with a gap size of 800 micrometers. The temperature was controlled in the rheometer through a peltier unit (Viscotherm VT2 Physica, Austria). The experimental data was fitted through the Carreau model:

$$\eta(t) = \eta_{\infty} + \frac{(\eta_O - \eta_{\infty})}{\left[1 + (\lambda \bullet \dot{\gamma})^2\right]^m} \tag{4}$$

where η_O represents the zero-shear rate or Newtonian viscosity, η_{∞} is the equilibrium viscosity at maximal shear rates, λ is the time constant corresponding to the Carreau model, and *m* is a dimensionless constant.

2.13. Atomic force microscopy (AFM)

Samples of each batch of NCC produced were separately dispersed in deionized water previously filtered through 25 microns nylon membranes (Micropore, USA). About 15 microliters of each suspension were dispersed on the corresponding mica sheet, and left for water evaporation into a desiccator. Also, 15 microliters of the water used for dispersions was deposited on mica sheets for control. Microscopy was then performed under a nitrogen atmosphere, by taking images with a cantilever through an atomic force microscope (NanoScope III, Digital Instruments, CA, USA) and performing image analysis [33] with the scanning probe microscopy

https://doi.org/10.1016/j.heliyon.2019.e01313

software WSxM 4.0 Develop 11.3-Package (2007, Nanotec Electronica, Spain). A total of nine samples, three from each of the three batches of NCC, were evaluated.

2.14. Statistical analysis

Extractions for each chemical analysis in WIF, MPH, AIR, AX-EF, and NCC were performed in triplicate ($n = 3$). Results were informed as the average and standard deviation for n replicates of each sample. An ANOVA (level of significance, $\alpha = 0.05$) followed by multiple comparisons evaluated through the least significant difference test was used to the analysis of results (Statgraphic Plus for Windows, version 5.0, 2001, Manugistic Inc., Rockville, MD, USA).

3. Results and discussion

3.1. Maize husk fibers

Dried husks milled through a cutting mill with a 500 μm mesh sieve produced a powder (MHP) characterized by the particle size distribution shown in Fig. 2A. The highest yield (55.4%) was obtained for 210 μm average particle size, though important proportions were also observed for 105 and 420 μm, and a significant yield for 53 μm.

Water activity of maize husk fiber varied between 0.253 and 0.285, being then stable during packaged storage in relation to lipid oxidation, hydrolytic reactions, non-enzymatic browning and microbial spoilage [34]. The MHP showed high lightness ($L^* \approx 78\%$), whereas the a^* color value was slightly negative, tending to green, and the b^* color value was well above zero ($\approx +25$) (Fig. 2B). Both a^* and b^* coordinates pointed to a yellow, slightly green, color.

3.2. Chemical composition

As reported in Table 1, a 31% of the MHP was water-soluble, and it was essentially constituted by reducing carbohydrates (85% w/w) and proteins (10.8%). In view of this composition, this water-soluble fraction can correspond to intracellular substances dissolved in the vacuoles and cytoplasm. As observed by Pengelly et al. [35], the outer husk surrounding the ear of maize has widely spaced veins with a number of interveinal mesophyll (M) cells. Big polyhedral cells similar to the M cells, orderly distributed like a palisade, contain a big vacuole that fills the intracellular space. In the husk operates the C_4 photosynthesis dispersed around the widely spaced veins in a diffusion-limited manner. GC analysis of the alditol acetates of the water-soluble fraction carbohydrates showed the presence of glucitol (two thirds) and mannitol (one third). A specific colorimetric analysis [19] indicated the presence of 29.0% of fructose (Table 1), suggesting that at least part of the mannitol and

https://doi.org/10.1016/j.heliyon.2019.e01313

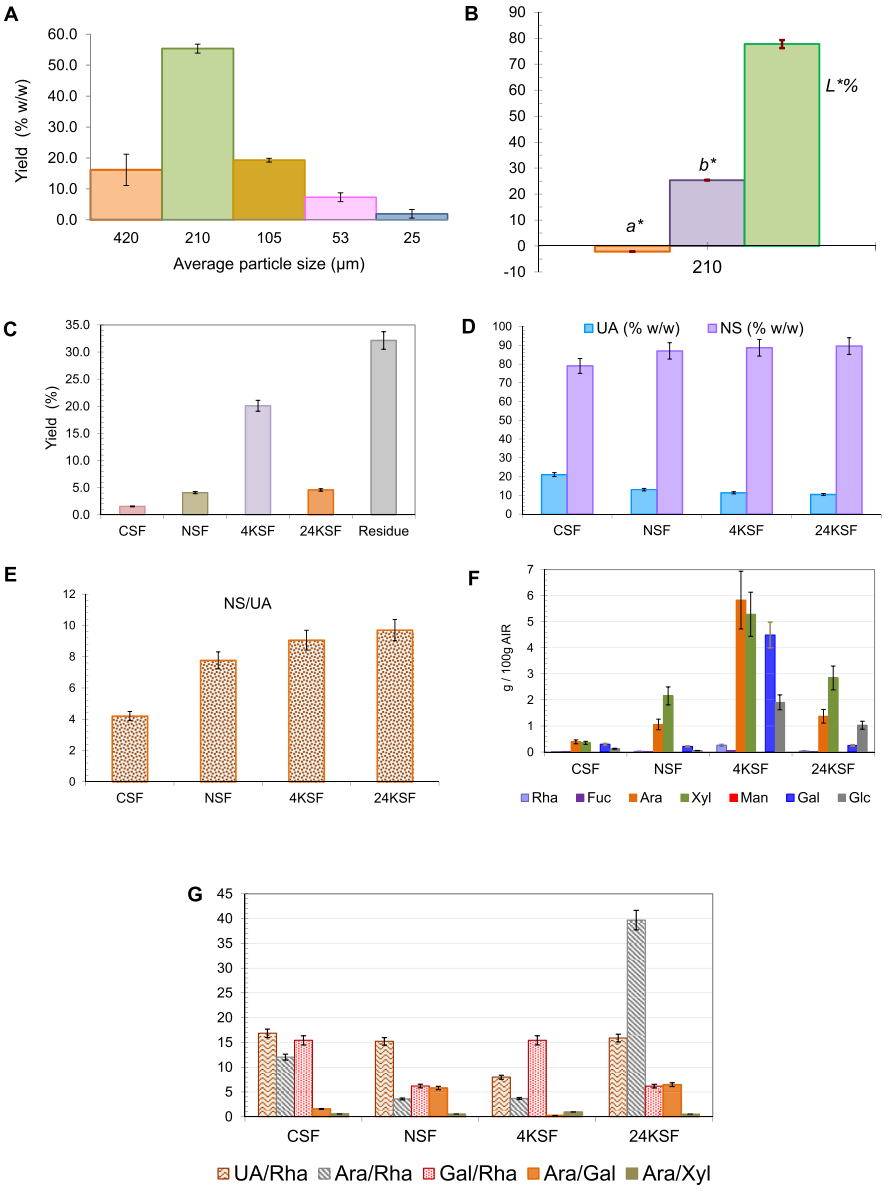

Fig. 2. Average particle size yields determined in maize husk powder (A). CIELab color parameters: *L** lightness, *a** and *b** color coordinates (B). Sequential extraction of cell wall polysaccharides: extraction yield of dissolved fractions (C); polysaccharide composition in UA and NS (D), and their molar ratio (E); NS composition of each extracted fraction: rhamnose (Rha), fucose (Fuc), arabinose (Ara), xylose (Xyl), mannose (Man), galactose (Gal) and glucose (Glc) contents (F); molar ratios calculated between NS components (G).

glucitol observed in the gas chromatogram becomes from fructose reduction. On the other hand, aldononitrile acetates from the 78% isopropanol-soluble subfraction showed the presence of glucononitrile and glucitol, indicating that the fraction contains both glucose and sorbitol (glucitol). This polyol has already been observed in maize extracts obtained from kernels [36]. This indicates that free glucose, fructose

https://doi.org/10.1016/j.heliyon.2019.e01313

Table 1. Yield[a] and chemical composition[a] of the maize husk powder (MHP) and arabinoxylan enriched fraction (AX-EF) extracted from the alcohol insoluble residue (AIR).

	Contents[a] (% w/w)
- Water soluble fraction yield with respect to MPH	31 ± 1
Reducing carbohydrates[b]	85 ± 1
Fructose	29 ± 1
Glucose	48 ± 1
Proteins	11 ± 1
- Alcohol insoluble residue (AIR) yield with respect to MPH	67 ± 3
Non-cellulosic polysaccharides[c,d]	57 ± 1
Proteins[d]	13.2 ± 0.6
Total starch[d]	<1
Cellulose[d]	26 ± 2
Lignin[d]	7 ± 1
Uronic acids[d,e]	5.0 ± 0.5
- AX-EF yield with respect to AIR	26 ± 2
Proteins[f]	6.1 ± 0.8
Total polysaccharides[c,f]	87 ± 1
Uronic acids[e,f]	3.9 ± 0.3
Rhamnose[f]	0.38 ± 0.06
Fucose[f]	ND
Arabinose[f]	21.3 ± 0.7
Xylose[f]	56 ± 1
Galactose[f]	1.9 ± 0.9
Glucose[f]	3.5 ± 1

[a] The mean and standard deviation ($n = 3$) are reported, and expressed on dry mass.
[b] Somogyi-Nelson's [14] spectrophotometric technique using D-fructose as standard.
[c] Determined through the method of Dubois et al. [15].
[d] Calculated on the AIR (dry) basis.
[e] Included into the non-cellulosic or total polysaccharides' contents.
[f] Calculated on the AX-EF (dry) basis. ND: non detectable.

and sorbitol constitute a major portion of the water-soluble fraction extracted from MHP. Through the enzymatic-colorimetric assay performed, a glucose content of 48% was confirmed in this fraction (Table 1).

The freeze-dried insoluble residue remaining after water extraction (WIF) was treated with 85% v/v ethanol and the alcohol insoluble fraction, AIR, was obtained with a yield of 67% with respect to the MHP dry mass. Hence, the WIF (70% yield) was almost totally constituted by the cell wall polymers (AIR) [37], which were essentially polysaccharides (83%) and proteins (Table 1). The latter can be ascribed

https://doi.org/10.1016/j.heliyon.2019.e01313

to hydroxyproline-rich glycoproteins (extensin) of the cell walls, as those reported to be crosslinked with pectins in cotton [38]. A 57% w/w of non-cellulosic polysaccharides, which included a low UA proportion corresponding to pectins (5.5%), and a high content of NS (≈52%) were found (Table 1). A 26% of cellulose and 0.58% of total starch were also determined in the AIR (Table 1). About a 7% of lignin was found (Table 1), which is a non-polysaccharide component of the secondary cell walls of vascular tissues [35, 37].

3.2.1. Sequential extraction of cell wall polymers

Besides the drying process, functional properties of fibers are mainly related to the polymeric composition as well as to the bioactive compounds present in the vegetable source [11, 39]. By the sequential extraction of the polymers that compose the cell wall material (AIR) isolated from the maize husks (Fig. 1) the crosslinks can be identified and, hence, the kind of polymers of which the maize husk is a source [40]. From this knowledge techniques can then be proposed for their extraction and usage.

According to the yields observed in Fig. 2C, pectins (CSF and NSF) and the hemicelluloses most firmly interacting with cellulose (24KSF) through hydrogen bonds [40] were the less significant components of maize husk cell walls.

Calcium- (CSF) and covalently (NSF) crosslinked pectins [40] were respectively constituted by 21% and 13% of UA (Fig. 2D), which mainly formed the homogalacturonan (HG) chains of pectins. A very high level of NS (79 and 87%; Fig. 2D) was found in both extracted fractions, which led to calculate NS/UA molar ratios of 4.2 and 7.8, respectively (Fig. 2E). These values were notably higher than those that usually correspond to pectins (≈1−2) [21]. Hence, it is suggested that the NS content can not be entirely assigned to pectins, but to soluble arabinoxylans since the highest NS levels corresponded to L-arabinose (Ara) and D-xylose (Xyl) (Fig. 2F). Ara/Xyl molar ratios of ≈1.8 and 0.7−0.8 were calculated for CSF and NSF, respectively (Fig. 2G).

There was much lower contents of L-rhamnose (Rha) (Fig. 2F) than of UA (Fig. 2D) in the CSF and NSF extracted pectins, showing UA/Rha molar ratios of 12.6−14 (Fig. 2G). Blocks of more than 10 unesterified UA (D-galacturonic acid, GalA) residues as herein calculated can yield pectins sensitive to Ca^{2+} crosslinking. HG chains are bound to the rhamnogalacturonan I (RG-I) cores known as hairy (amorphous) regions because of the lateral substitution by arabinogalactan side chains [41]. Rha units of the RG-I seemed to be substituted by a higher proportion of Ara (Ara/Rha) than of D-galactose (Gal) (Gal/Rha) in CSF and NSF (Fig. 2G). However, the highest proportion of the Ara corresponded to arabinoxylans. In commelinid monocots (which include grasses and some related species like maize), xylans are the major non-cellulosic polysaccharides in their primary cell walls, constituting

https://doi.org/10.1016/j.heliyon.2019.e01313

about 20% of them. These xylans usually contain many Ara residues attached to the backbone, being then known as arabinoxylans [42].

The final residue of the sequential extraction (Fig. 1), which included cellulose and lignin, was one of the two major components determined in maize husk cell walls (Fig. 2C), and cellulose was specifically the main polymer found in this residue through the selective extraction with sulfuric acid (Table 1). Hemicelluloses less retained by cellulose (4KSF) constituted the other main component of maize husks (Fig. 2C). This fraction showed the highest contents found for Xyl and Ara (Fig. 2F), which certainly contributed to the NS content (Fig. 2D). They can correspond to insoluble arabinoxylans since a low Ara substitution (Ara/Xyl) was determined (Fig. 2G). According to the yield of 24KSF, only a low level of hemicelluloses was highly retained by cellulose in maize husks (Fig. 2C), being then insoluble arabinoxylans (Fig. 2F) as inferred from the low substitution by Ara (Fig. 2G). According to Ebringerová et al. [43], the degree of substitution of xylans by Ara affects the solubility of the arabinoxylans. They are classified into two or three groups, depending on the isolation and fractionation procedures as well as on the distribution patterns of substitution by the Ara residues. The first group includes water-insoluble monosubstituted arabinoxylans (Ara/Xyl up to 0.2−0.3), similar to the ratio found for 4KSF, with α-L-Ara*f* moieties attached mainly at position 3 of the β 1→4 xylan backbone. The second and third groups comprise water-soluble xylans with 0.3−1.2 Ara/Xyl molar ratios. Arabinoxylans of the second group, with intermediate Ara/Xyl molar ratios (0.5−0.9) have shorter sequences of disubstituted Xyl*p* residues than those of the third group. As reported by these authors, the alkali-extractable arabinoxylans are of particular interest as they could have similar but stronger bread-improving properties than the water-extractable arabinoxylans for the baking performance of cereal flours.

Residual amounts of pectins (Fig. 2D), physically entangled in the hemicellulose-cellulose network through arabinogalactan side chains [44], were also isolated with the hemicelluloses (4KSF and 24KSF). This was inferred because around 10% of remaining UA was found in 4KSF and 24KSF (Fig. 2D), together with some residual content of Rha (Fig. 2F). Gal was also found in 4KSF and 24KSF (Fig. 2F) as well as significant Gal/Rha molar ratios (Fig. 2G) for these pectins.

Glucose units (Glc) were also determined in the NS of 4KSF and 24KSF (Fig. 2F). In grass cell walls, the sources of Ara and Xyl are primarily the arabinoxylans, but xyloglucans could also contribute to the Glc content [42, 45].

3.2.2. Phenolic compounds

The extractable phenolics were directly obtained from the MHP by water/acetic acid/acetone (Table 2). By considering the UV wavelength of absorption, these phenolics

https://doi.org/10.1016/j.heliyon.2019.e01313

Table 2. HPLC-DAD and HPLC-ESIMS results of the maize husk powder (MHP) extractable (coumaric and cinnamic acids-contents) and esterified phenolic compounds (ferulic acid monomer, and dimeric and trimeric forms).

Phenolic compounds	Peak number	HPLC retention time (min)	HPLC-UV-DAD (nm)	HPLC-ESIMS (m/z)	mg/100 g of MHP[a]
Extractable phenolic compounds					
Coumaric acids[b]	3	28	318		<1
	5	32	309		<1
	9	47	310		1.27 ± 0.08
Cinnamic acids[c]	2	23	328		<1
	7	35	325		<1
	8	41	334		<1
	10	48	322		<1
	12	50	337		1.0 ± 0.1
	13	52	333		<1
	14	57	327		0.93 ± 0.06
	15	62	320		<1
	16	64	328	542[d]	7.5 ± 2
Esterified phenolic compounds[e]					
Ferulic acid monomer	1	40	308	193	6.1 ± 0.8
Ferulic acid dimers	3	42	322	385	8.1 ± 0.2
	6	55	324	385	1.5 ± 0.1
Ferulic acid trimers	7	58	324	563	1.7 ± 0.1
	8	59	323	563	1.2 ± 0.1

[a] The mean and standard deviation ($n = 3$) are reported.

[b] Quantified as cholorogenic acid (5-O-caffeoylquinic acid).

[c] Quantified as cinnamic acid.

[d] Caffeoyl-dimethoxy-cinnamoyl quinic acid.

[e] Quantified as ferulic acid (4-hydroxy-3-methoxycinnamic acid).

belonged to the coumaric acid and cinnamic acid groups (Table 2). The coumaric acids showed three main components that maximally absorbed between 309 and 318 nm, with retention times of 28, 32 and 47 min. The cinnamic acid group presented nine main components that absorbed between 320 and 337 nm, with retention times between 23 and 64 min (Table 2). The total content of the coumaric acids was 2.8 mg/100 g of MHP (Table 2). On the other hand, the caffeoyl-dimethoxy-cinnamoyl quinic acid was identified by its $[M-H]^-$ at m/z 542 as the major component of the cinnamic acid derivatives found, with a content of 7.45 mg/100 g MHP (Table 2). The rest of the cinnamic acids were present in amounts in general lower than 1 mg/100 g MHP. All of these extractable phenolics can have in part an intracellular origin and/or were non-covalently bound to the cell wall polysaccharides. According to that summarized in Table 2, the total content of extractable phenolics was 13.78 mg/100 g MHP.

After an alkaline pre-treatment, the phenolic compounds retained through covalent bonds by the cell wall polymers were liberated by hydrolysis. Considering the UV wavelength of absorption and the ions obtained and analyzed through HPLC-ESI-MS, the ferulic acid (40 min retention time) and its dimeric form with 42 min of

https://doi.org/10.1016/j.heliyon.2019.e01313

retention time were mostly released (Table 2). Their respective contents were 6.14 and 8.10 mg/100 g MHP. As reported in Table 2, a second isomer of the ferulic acid dimeric form with a retention time of 55 min, as well as two isomers of the ferulic acid trimer were also determined, though in low concentrations (1.2−1.68 mg/100 g MHP). As can then be calculated from that reported in Table 2, the total content of ferulic acid was 18.64 mg/100 g MHP. The O-3 of the Ara residues of arabinoxylans and also of pectins can be esterified to the carboxylic group of the ferulic acid residue, contributing to the insolubilization of these polysaccharides [46].

3.2.3. Carotenes and antioxidant capacity

MHP contained carotenes, which can be associated to the MPH color. Carotenes remained concentrated in the WIF (Table 3). Conversely, the AIR showed lower carotene content than the other two fractions because of the ethanolic extraction of this fraction (Table 3). β-Carotene, β-cryptoxanthin, zeaxanthin and lutein were found by Žilić et al. [47] as the predominant carotenoids in the case of maize kernels.

MHP showed an important antioxidant capacity when evaluated in its radical scavenging (DPPH assay) and reducing (FRAP assay) activities, expressed as L-(+)-ascorbic acid (Table 3). However, the significantly lower antioxidant capacity of the WIF and of AIR did not correlate with their respective levels of carotenes. From these results, it may be inferred that the extractable phenolics contained in the MHP (Table 2) can mainly contribute to the antioxidant capacity (Table 3). The low antioxidant activity of the WIF and AIR can be ascribed to the fact that their phenolics are mainly bound or esterified (Table 2) and can then not contribute significantly to the antioxidant capacity. Pulido et al. [30] suggested that the hydroxylation and conjugation degrees seemed to determine the reducing power of Fe^{3+} by polyphenols, while the carotenoids did not show reducing activity *in vitro*. Gil et al. [48]

Table 3. Content of carotenes and antioxidant activity of maize husk isolated fibers.

	Carotenes (mg/100 g)[a,b]	DPPH (mg/100 g)[a,c]	FRAP (mg/100 g)[a,c]
Maize husk powder (MHP)	4 ± 1^{A}	190 ± 1^{A}	206 ± 9^{A}
Water insoluble maize husk fiber (WIF)	6 ± 1^{B}	34 ± 1^{B}	25 ± 1^{B}
Alcohol insoluble residue (AIR): cell wall components	$<2^{C}$	21 ± 2^{C}	15 ± 3^{C}

[a] Reported as the mean and standard deviation ($n = 3$), and expressed on dry mass of MPH, WIF, or AIR, as appropriate. The same capital letters as superscripts in a column mean non-significant differences ($p < 0.05$).

[b] Expressed as beta-carotene.

[c] Expressed as L-(+)-ascorbic acid.

https://doi.org/10.1016/j.heliyon.2019.e01313

determined that the phenolic compounds showed a much higher contribution to the antioxidant activity measured through the DPPH and FRAP assays than the carotenoids when determined in plums, peaches, and nectarines harvested in California. Also found a strong correlation between the total phenolic contents and the antioxidant activity in these fruits.

3.3. Maize husks as a source of fibers

By considering the results obtained from the sequential extraction concerning the yields (Fig. 2C) and polysaccharide composition (Fig. 2F), as well as the existence of ferulate bridges (Table 2), an alkaline hydrolysis with KOH 4% (24 h, 23 °C) was then performed directly on the AIR in order to isolate a fraction enriched in the more extractable arabinoxylans of the 4KSF, which also can include co-extracted calcium-(CSF) and covalently (NSF) crosslinked pectins (Fig. 1). In a similar way, considering the residue's yield shown in Fig. 2C, and its chemical composition in cellulose together with the low level of lignin (Table 1), an acid hydrolysis with sulfuric acid (64% w/w) was directly carried out on the AIR to extract a fiber enriched in crystalline cellulose without applying a previous delignification process.

3.3.1. Alkaline hydrolysis of AIR: arabinoxylans-enriched fraction (AX-EF)

The alkaline soluble fraction of fiber recovered after insolubilization in ethanol followed by filtration and drying (see section 2.2.1) was obtained with a yield of 26% (Table 1). It was essentially constituted by polysaccharides (87%), which included a 3.9% of uronic acids ascribed to pectins. Also, a 6.1% of cell wall proteins was determined. As reported in Table 1, the composition of NS determined through GC shows that arabinoxylans were the main components of the AX-EF, since a 55.6% was Xyl and a 21.3% was Ara. An Ara/Xyl molar ratio of 0.38 was then obtained, value which is in the limit between the mono-substituted water insoluble and water-soluble arabinoxylans, according to that indicated by Ebringerová et al. [43]. Only residual contents of Rha and Gal, associated to the RG-I of pectins, and Glc were found (Table 1).

The flow rheological behavior of the 2.00% w/v aqueous solution of AX-EF, either without or with calcium ions (30 mg/g UA), was determined at 20.0 °C by recording the viscosity as a function of the shear rate up to 200 s^{-1} in a rheometer, for 50 min (Fig. 3A). The same assay was performed for comparison on the 4KFS fraction (Fig. 3B), whose composition was reported in Fig. 2. All of these solutions presented pseudoplastic behavior since the viscosity decreased with the increment in shear rate from the Newtonian region of constant viscosity (η_O) at the lowest shear rates, to the limit viscosity (η_∞) at the highest shear rate values (Fig. 3A and B). This behavior corresponds to flexible hydrated macromolecules or random coil polymers which

https://doi.org/10.1016/j.heliyon.2019.e01313

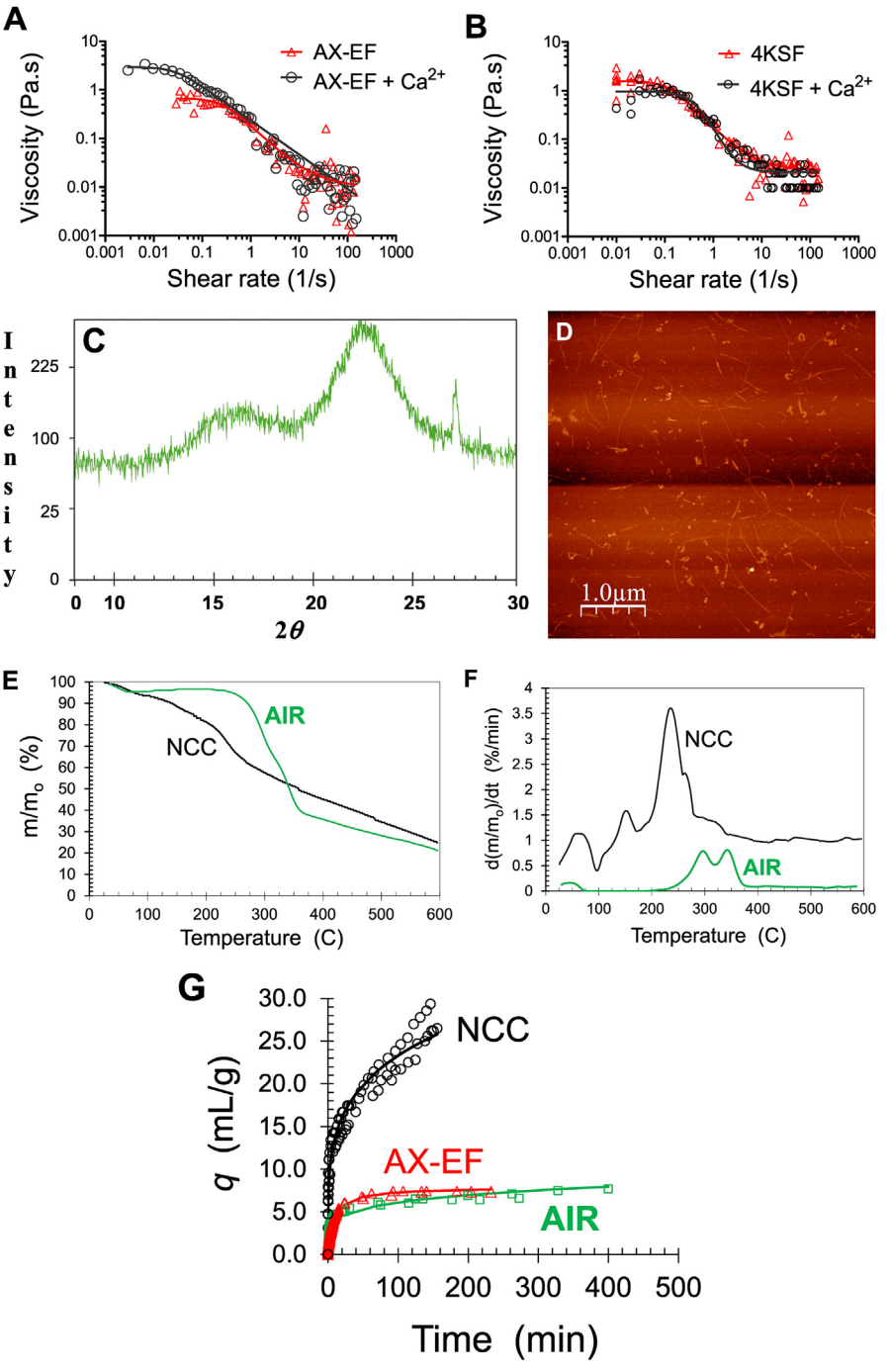

Fig. 3. Viscosity curves recorded at 20.0 °C from AX-EF (A) and 4KSF (B) 2.00% w/v aqueous solutions without or with calcium (30 mg Ca^{2+}/g GalA); continuous lines correspond to the Carreau's model fitted. X-ray diffraction pattern of NCC (C); AFM image obtained from NCC; bar = 1.0 μm (D). Thermogravimetry: mass loss (E) and the corresponding derivative, DTG, (F) curves. Kinetics of water absorption of the AIR source, and of NCC and AX-EF (G).

https://doi.org/10.1016/j.heliyon.2019.e01313

interact through entanglements and, hence, a network structure is formed in water at rest [49, 50]. When the shear rates just increased above a critic value, the viscosity began to decrease gradually because the shear rates applied are higher than the velocity by which the polysaccharides can form new entanglements for interaction, and the network is then being destroyed up to reach the limit or minimal viscosity (η_∞). Calcium ions increased significantly the Newtonian viscosity (η_O) for the AX-EF solution, which showed the highest value of η_O, showing the most structured network where the η_∞ is not observed. The sensibility of the AX-EF to calcium ions can be explained by the pectins (uronic acid content) (Table 1). Though this fraction had lower content of pectins than that of the 4KFS, probably they had the minimal amount of uronic acid residues required into the HG blocks to form calcium bridges and the egg-box like structure [41].

3.3.2. Acid hydrolysis of AIR: fraction enriched in crystalline cellulose (NCC)

The treatment of the AIR with 64% (w/w) sulfuric acid (section 2.2.2) permitted to obtain an NCC fraction with a yield of 26% (Table 4). Its elemental composition demonstrated a 1.250% w/w of sulfur content, indicating that sulfated cellulose at the hydroxyl groups was obtained (Table 4). According to the abundance of each element in relation to sulfur, one sulfate group every 14 glucose residues of the cellulose macromolecules in the NCC fraction can be calculated (Table 4). Neto et al. [51] determined a concentration of sulfate groups of 111 mmoles/kg of cellulose or

Table 4. Yield[a] and elemental composition[a] of the NCC fraction extracted from the AIR. The zeta potential (*Zp*) is also summarized.

Yield (g/100 g AIR)	26 ± 5	
Elemental analysis		
Element	% (w/w)[a,b]	Abundance relative to sulfur
C	40 ± 1	86.0
H	5 ± 1	125
S	1.2 ± 1	1.0
O	54 ± 1	86
Zp[a] (mV)		−15 ± 2
	Diameter (nm)	Length (nm)
Size[c]	28 ± 9	1452 ± 1014

[a] The mean and standard deviation ($n = 3$) are reported.

[b] Expressed on dry mass.

[c] Measured on the AFM images. The mean and standard deviation ($n = 9$) are reported.

https://doi.org/10.1016/j.heliyon.2019.e01313

about 0.40% w/w of sulfur in crystalline nanocellulose extracted through acid hydrolysis from the shell of soybeans. Differences in the sulfated degree can be also due to differences in the dialysis procedure, since it promotes de-sulfation in the surface of nanocrystals [52].

The zeta potential measured in water was −15 mV, which results from the negatively charged sulfate groups (Table 4). Absolute values lower than 15 mV (negatives or positives) induce particles' agglomeration while those above 30 mV make that the repulsion predominates and the colloidal system obtained by dispersion in water can then be stable [53]. Higher sulfuric acid concentrations or especially longer reaction times can increase the proportion of sulfated hydroxyl groups in the cellulose [54].

The X-ray diffraction study of NCC indicated an amorphous profile with a main diffraction peak next to $2\theta \approx 22.00°$ ($d \approx 4.05$ Å; Eq. (3)) together with other signal at $2\theta \approx 15.00°$ ($d \approx 5.88$ Å) (Fig. 3C), respectively attributable to typical reflection planes of type I cellulose, 002 and 101 [55, 56]. In addition, a region between $2\theta \approx 12°$ and 18° associated to the amorphous phase of the natural polymer is observed, which is due to the low order in the carbohydrate chains [57]. A 56% of crystallinity was determined in the NCC fraction. This is coherent with that observed through the AFM images shown in Fig. 3D, where two populations of particles were observed: the cellulose fibrils (28 nm diameter and 1452 nm length), that contributed with a higher proportion of amorphous material revealed by the X-ray diffraction analysis, and the small particles of crystalline nanocellulose. The chemical treatments can alter the structure order, being possible to reach for example a higher degree of crystallinity by elimination of the amorphous regions in cellulose through alkaline pretreatments [58].

Under nitrogen, the TGA profiles were recorded from the NCC as well as from the cell wall polymers (AIR) used for production of the NCC (Fig. 3E and F). An initial mass loss of ≈4% produced up to ≈90 °C was observed for both NCC and AIR, which can be ascribed to water evaporation (Fig. 3E). The inflexion points were revealed by the peaks in the calculated DTG profile (Fig. 3F), which corresponded to degradation temperatures. They were observed for the NCC at 147 °C and mainly at 232° and 257 °C, with a higher mass loss. However, the thermal decomposition temperatures of the AIR were 294 °C and 344 °C (Fig. 3F), both higher than those determined for the NCC. Lignin probably followed with its decomposition beyond 344 °C. The NCC had a residual mass of 24.8% while the AIR left a 19% (Fig. 3E). Roman and Winter [54] studied the thermal decomposition of bacterial cellulose which showed similar behavior to that observed for the NCC fraction, being concluded by the authors that the sulfate groups were responsible for both the lower thermal stability of the cellulose fractions produced, and the increase in the char fraction, confirming that the sulfate groups act as flame retardants.

https://doi.org/10.1016/j.heliyon.2019.e01313

3.3.3. Kinetics of spontaneous water absorption of the AX-EF and NCC

The functional performance of vegetable fibers is associated to their hydration properties, which are related to the polysaccharide composition and drying process [39]. Fig. 3G shows the kinetic curves of spontaneous water absorption by the AX-EF and NCC, together with that of the AIR used for their production, which was included for comparison. The highest velocity and maximal water absorption was shown by the NCC material, whereas the AX-EF presented a curve of the same order of magnitude than that of the AIR. The kinetic curve of the AX-EF reached the equilibrium after 90 min, while the absorption curves of the NCC and AIR were different, increasing continuously (Fig. 3G). As a consequence, the AX-EF experimental points were only adequately fitted by the Boquet's model ($R^2 = 0.971$; Eq. (2)), while the NCC and AIR ones fitted to the Ritger and Peppas' power law model ($R^2 = 0.958-0.938$; Eq. (1)) corresponding to polymers that swells in the solvent either through a Fickian or an anomalous mechanism [12]. Since the n exponent values of Eq. (1) were similar (0.231 ± 0.007 and 0.189 ± 0.008), the comparison of the rate constants of water absorption (k) demonstrated that the NCC material enriched in crystalline cellulose absorbed water three times more rapidly ($k = 8.0 \pm 0.2$ $mL \cdot g^{-1} \cdot min^{-0.231}$) than the AIR ($k = 2.56 \pm 0.09$ $mL \cdot g^{-1} \cdot min^{-0.189}$), which is constituted by the cell wall polymers (Table 1). On the other hand, the AX-EF showed a maximal water absorption capacity of 7.9 ± 0.1 mL/g, being 8.4 ± 0.3 min the time needed to reach a half of the maximal water absorption capacity (Eq. (2)). The arabinoxylans that mainly constituted the AX-EF (Table 4) seemed to have limited swelling and then narrow absorption capacity of water, whereas the isolated crystalline cellulose of the NCC and AIR were able to swell continuously and then to absorb relatively unlimited amounts of water (Fig. 3G). However, the drying procedure also affects the absorption capacity of powders, which also involves a capillary suction phenomenon. Hence, the porosity is an important characteristic of the material in this sense. NCC and AIR were freeze-dried, whereas the AX-EF was dried by evaporation at room temperature under convection.

4. Conclusions

The maize husk powder (MPH) was constituted by a 31% of water soluble material of which 10.8% were proteins and 85% were monosaccharides (fructose and glucose) and sorbitol, being probably the intracellular content of the mesophyll cells of the maize husks. Carotenes ($\approx$5 mg/100 g MPH) and extractable phenolics ($\approx$14 mg/100gMHP of coumaric and cinnamic acids like caffeoyl-dimethoxy-cinnamoyl quinic acid) were found, being these phenolics which mainly contributed to the high antioxidant capacity (200 mg ascorbic acid/100 g MPH or WIF). Also, bound ferulic acid residues (monomer, dimers and trimers) were found by alkaline

https://doi.org/10.1016/j.heliyon.2019.e01313

hydrolysis. The remaining WIF (69% of the MPH) was almost totally composed by the cell wall polymers or the AIR fraction (67% of the MPH). They were mainly less retained arabinoxylans (20%), together with cellulose (26%), and only a 5.5% of pectins and lignin (7%). The latter made this derivative able to material development because delignification can be avoided for cellulose isolation. By considering all these results, a 1.25% of sulfur (sulfated) nanocellulose (NCC) and a water soluble AX-EF with pseudoplastic behavior in water at a 2% w/v concentration, and sensible to Ca^{2+}, reaching 3 Pa•s of Newtonian viscosity, were respectively obtained. NCC was constituted by 28-nm width nanofibers and smaller nanoparticles. The sulfate groups were responsible for both the lower thermal stability of the NCC (147 °C onset), and the increase in the char fraction, in comparison to the AIR. Despite a 56% of crystallinity, the NCC showed by far the highest water absorption velocity and capacity when compared to those of the AX-EF and AIR.

Maize husks constitute a source of functional food additives and materials with relevant hydration properties and antioxidant capacity. The potential of maize husk as a useful carbon source of chemicals can diversify the farmers' and industry productions, constituting a new source of income.

Declarations

Author contribution statement

Dana C. Bernhardt, Nora M. A. Ponce, Maria F. Basanta: Performed the experiments; Analyzed and interpreted the data.

Carlos A. Stortz: Conceived and designed the experiments; Analyzed and interpreted the data; Contributed reagents, materials, analysis tools or data.

Ana M. Rojas: Conceived and designed the experiments; Analyzed and interpreted the data; Contributed reagents, materials, analysis tools or data; Wrote the paper.

Funding statement

This work was supported by the University of Buenos Aires [UBACyT 2014−2017 20020130100553BA], Agencia Nacional de Promoción Científica y Tecnológica de la República Argentina (ANPCyT) [PICT 2013−2088, 2015−2109].

Competing interest statement

The authors declare no conflict of interest.

Additional information

No additional information is available for this paper.

https://doi.org/10.1016/j.heliyon.2019.e01313

Acknowledgements

We also thank National Research Council of Argentina (CONICET), and Eng. Delorenzi (INTI-Celulosa y Papel, Buenos Aires, Argentina).

References

[1] L. Gibson, G. Benson, Origin, History, and Uses of maize (*Zea mays*), 2002. http://agron-www.agron.iastate.edu/Courses/agron212/readings/maize_history.htm.

[2] K.S. Dhugga, Maize biomass yield and composition for biofuels, Crop Sci. 47 (2007) 2211−2227.

[3] G. Roth, Maize Stover for Biofuel Production, 2015. http://www.extension.org/pages/26618/maize-stover-for-biofuel-production#.VTL8mtJ_Oko.

[4] X. Hernández, Caen las estimaciones de la cosecha 2017/2018, se prevén 46,5 Mt de soja y 35 Mt de maíz, 2018. Infocampo.com.ar, http://www.infocampo.com.ar/cen-las-estimaciones-de-la-cosecha-20172018-se-preven-465-mt-de-soja-y-35-mt-de-maiz/.

[5] A. Olagunju, E. Onyike, A. Muhammad, S. Aliyu, A.S. Abdullahi, Effects of fungal (*Lachnocladium* spp.) pretreatment on nutrient and antinutrient composition of maize cobs, Afr. J. Biochem. Res. 7 (11) (2013) 210−214.

[6] COST European Cooperation in Science and Technology Project, TD1203-Food Waste Valorisation for Sustainable Chemicals, Materials & Fuels, EU-Bis), 2013−2014, p. 207., at: costeubis.org/.

[7] M.J. John, S. Thomas, Biofibres and biocomposites, Carbohydr. Polym. 71 (2008) 343−364.

[8] Stockholm, Sweden, International Foundation for Science, Annual Report, 2010, http://www.ifs.se/IFS/Documents/Publications/Annual%20reports/IFS%20Annual%20Report%202010.pdf.

[9] T.K. Fagbemigun, O.D. Fagbemi, O. Otitoju, E. Mgbachiuzor, C.C. Igwe, Pulp and paper-making potential of maize husk, Int. J. Agric. Sci. 4 (4) (2014) 209−213.

[10] Z. Kohajdová, J. Karovičová, M. Jurasová, Influence of carrot pomace powder on the rheological characteristics of wheat flour dough and on wheat rolls quality, Acta Sci. Polon. Techn. Alimen. 11 (2012) 381−387.

https://doi.org/10.1016/j.heliyon.2019.e01313

[11] M.F. de Escalada Pla, A.M. Rojas, L.N. Gerschenson, Effect of butternut (*Cucurbita moschata* Duchesne ex Poiret) fibres on bread-making, quality and staling, Food Bioproc. Technol. 6 (2013) 828−838.

[12] M.F. Basanta, M.F. de Escalada Pla, M.D. Raffo, C.A. Stortz, A.M. Rojas, Cherry fibers isolated from harvest residues as valuable dietary fiber and functional food ingredients, J. Food Eng. 126 (2014) 149−155.

[13] M. Elleuch, D. Bedigian, O. Roiseux, S. Besbes, Ch. Blecker, H. Attia, Dietary fibre and fibre-rich by-products of food processing: characterization, technological functionality and commercial applications: a review, Food Chem. 124 (2011) 411−421.

[14] N. Nelson, A photometric adaptation of the Somogyi method for the determination of glucose, J. Biol. Chem. 153 (1944) 375−380.

[15] M. Dubois, K.A. Gilles, J.K. Hamilton, P.A. Robers, F. Smith, Colorimetric method for determination of sugars and related substances, Anal. Chem. 28 (1956) 350−356.

[16] T.M.C.C. Filisetti-Cozzi, N.C. Carpita, Measurement of uronic acids without interference from neutral sugars, Anal. Biochem. 197 (1991) 157−162.

[17] O.H. Lowry, N.J. Rosebrough, A.L. Farr, R.J. Randall, Protein measurement with the Folin phenol reagent, J. Biol. Chem. 193 (1) (1951) 265−275.

[18] R. Mattoo, M. Ishaq, M. Saleemuddin, Protein assay by Coomassie Brilliant Blue G-250 binding methods unsuitable for plant tissues rich in phenols and phenolases, Anal. Biochem. 163 (1987) 376−384.

[19] W. Yaphe, G.P. Arsenault, Improved resorcinol reagent for the determination of fructose, and of 3,6-anhydrogalactose in polysaccharides, Anal. Biochem. 13 (1965) 143−148.

[20] E.N. Fissore, N.M.A. Ponce, L. Matkovic, C.A. Stortz, A.M. Rojas, L.N. Gerschenson, Isolation of pectin enriched products from red beet (*Beta vulgaris* L. var. conditiva) wastes: composition and functional properties, Food Sci. Technol. Int. 17 (6) (2011) 517−527.

[21] M.F. Basanta, M.F. de Escalada Pla, C.A. Stortz, A.M. Rojas, Chemical and functional properties of cell wall polymers from two cherry varieties at two developmental stages, Carbohyd. Polym. 92 (2013) 830−841.

[22] L. Brinchi, F. Cotana, E. Fortunati, J.M. Kenny, Production of nanocrystalline cellulose from lignocellulosic biomass: technology and applications, Carbohydr. Polym. 94 (1) (2013) 154−169.

https://doi.org/10.1016/j.heliyon.2019.e01313

[23] J.P. Saraiva Morais, M. de Freitas Rosa, M. de sá Moreira de Souza Filho, L. Dias Nascimento, D. Magalhães do Nascimento, A. Ribeiro Cassales, Extraction and characterization of nanocellulose structures from raw cotton linter, Carbohydr. Polym. 91 (2013) 229–235.

[24] A.K. Biswas, J. Sahoo, M.K. Chatli, A simple UV-Vis spectrophotometric method for determination of b-carotene content in raw carrot, sweet potato and supplemented chicken meat nuggets, LWT Food Sci. Technol. 44 (2011) 1809–1813.

[25] J.J. Karkalas, An improved enzymic method for the determination of native and modified starch, J. Sci. Food Agric. 36 (1985) 1019–1027.

[26] A. Ng, A.J. Parr, L.M. Ingham, N.M. Rigby, K.M. Waldron, Cell wall chemistry of carrots (*Daucus carota* CV. Amstrong) during maturation and storage, J. Agric. Food Chem. 46 (1998) 2933–2939.

[27] M.F. Basanta, A. Marin, S.A. De Leo, L.N. Gerschenson, A.G. Erlejman, F.A. Tomás-Barberán, A.M. Rojas, Antioxidant Japanese plum (*Prunus salicina*) microparticles with potential for food preservation, J. Funct. Foods 24 (2016) 287–296.

[28] S. Vaidyanathan, M. Bunzel, Development and application of a methodology to determine free ferulic acid and ferulic acid ester-linked to different types of carbohydrates in cereal products, Cereal Chem. 89 (5) (2012) 247–254.

[29] W. Brand-Williams, M.E. Cuvelier, C. Berset, Use of a free radical method to evaluate antioxidant activity, LWT Food Sci. Technol. 28 (1995) 25–30.

[30] R. Pulido, L. Bravo, F. Saura-Calixto, Antioxidant activity of dietary polyphenols as determined by a modified ferric reducing/antioxidant power assay, J. Agric. Food Chem. 48 (2000) 3396–3402.

[31] L.P. Xiao, Z.J. Sun, Z.J. Shi, F. Xu, R.C. Sun, Impact of hot compressed water pretreatment on the structural changes of woody biomass for bioethanol production, BioResources 6 (2) (2011) 1576–1598.

[32] M.G. Carneiro-da-Cunha, M.A. Cerqueira, B.W.S. Souza, J.A. Teixeira, A.A. Vicente, Influence of concentration, ionic strength and pH on zeta potential and mean hydrodynamic diameter of edible polysaccharide solutions envisaged for multinanolayered films production, Carbohydr. Polym. 85 (3) (2011) 522–528.

[33] I. Horcas, R. Fernandez, J.M. Gomez-Rodriguez, J. Colchero, WSXM: a software for scanning probe microscopy and a tool for nanotechnology, Rev. Sci. Instr. 78 (2007) 013705.

https://doi.org/10.1016/j.heliyon.2019.e01313

[34] T.P. Labuza, L. McNally, D. Gallagher, J. Hawkes, F. Hurtado, Stability of intermediate moisture foods. 1. Lipid oxidation, J. Food Sci. 37 (1972) 154−159.

[35] J.J.L. Pengelly, S. Kwasny, S. Bala, J.R. Evans, E.V. Voznesenskaya, N.K. Koteyeva, G.E. Edwards, R.T. Furbank, S. von Caemmerer, Functional analysis of maize husk photosynthesis, Plant Phys. 156 (2011) 503−513.

[36] J.R. Shaw, D.B. Dickinson, Studies on sugars and sorbitol in developing maize kernels, Plant Phys. 75 (1984) 207−211.

[37] C.T. Brett, K.W. Waldron, The Physiology and Biochemistry of Plant Cell walls, Chapman and Hall, London, 1996, 128, 133, 162.

[38] X. Qi, B.X. Behrens, P.R. West, A.J. Mort, Solubilization and partial characterization of extensin fragments from cell wall of cotton suspension cultures, Plant Phys. 108 (1995) 1691−1701.

[39] M.F. Basanta, S.R. Rizzo, N. Szerman, S.R. Vaudagna, M.A. Descalzo, L.N. Gerschenson, C.D. Pérez, A.M. Rojas, Plum (*Prunus salicina*) peel and pulp microparticles as natural antioxidant additives in breast chicken patties, Food Res. Int. 106 (2018) 1086−1094.

[40] S.C. Fry, Cross-linking of matrix polymers in the growing cell walls of angiosperms, Ann. Rev. Plant Phys. 37 (1986) 165−186.

[41] J.P. Vincken, H.A. Scholsm, R.J.F.J. Oomen, M.C. McCann, P. Ulvskov, A.G.J. Voragen, R.G. Visser, If homogalacturonan were a side chain of rhamnogalacturonan I. Implications for cell wall architecture, Plant Phys. 132 (2003) 1781−1789.

[42] H.V. Scheller, P. Ulvskov, Hemicelluloses, Ann. Rev. Plant Biol. 61 (2010) 263−289.

[43] A. Ebringerová, Z. Hromádková, T. Heinze, Hemicellulose, Adv. Polym. Sci. 186 (2005) 1−67.

[44] A.W. Zykwinska, M.C.J. Ralet, C.D. Garnier, J.F.J. Thibault, Evidence for in vitro binding of pectin side chains to cellulose, Plant Phys. 139 (1) (2005) 397−407.

[45] D.M. Rancour, J.M. Marita, R.D. Hatfield, Cell wall composition throughout development for the model grass *Brachypodium distachyon*, Front. Plant Sci. 3 (2012) article 266 1−14.

[46] E. Dornez, K. Gebruers, J. Delcour, C. Courtin, Grain-associated xylanases: occurrence, variability, and implications for cereal processing, Trends Food Sci. Technol. 20 (2009) 495−510.

https://doi.org/10.1016/j.heliyon.2019.e01313

[47] S. Žilić, V. Hadži-Tašković Šukalović, M. Milašinović, D. Ignjatović-Micić, M. Maksimović, V. Semenčenko, Effect of micronisation on the composition and properties of the flour from white, yellow and red maize, Food Technol. Biotechnol. 48 (2) (2010) 198−206. FTB-2320.

[48] M.I. Gil, F.A. Tomás-Barberán, B. Hess-Pierce, A. Kader, Antioxidant capacities, phenolic compounds, carotenoids, and vitamin C contents of nectarine, peach, and plum cultivars from California, J. Agric. Food Chem. 50 (17) (2002) 4976−4982.

[49] S.B. Ross-Murphy, Rheological methods, in: S.B. Ross-Murphy (Ed.), Physical Techniques for the Study of Food Biopolymers, Blackie Academic & Professional, Chapman & Hall, London, 1994, pp. 343−393.

[50] S. Lee, K. Warner, G.E. Inglett, Rheological properties and baking performance of new oat beta-glucan-rich hydrocolloids, J. Agric. Food Chem. 53 (2005) 9805−9809.

[51] W.P.F. Neto, H.A. Silvério, N.O. Dantas, D. Pasquini, Extraction and characterization of cellulose nanocrystals from agro-industrial residue − Soy hulls, Ind. Crops Prod. 42 (2013) 480−488.

[52] N. Wang, E. Ding, R. Chen, Thermal degradation behaviors of spherical cellulose nanocrystals with sulfate groups, Polymer 48 (12) (2007) 3486−3493.

[53] F.M. Tiller, W. Li, W. Chen, Solid/liquid separation, in: L. Albright (Ed.), Albright's Chemical Engineering Handbook, CRC Press, Boca Raton (FL), 2008, pp. 1597−1666.

[54] M. Roman, W.T. Winter, Effect of sulfate groups from sulfuric acid hydrolysis on the thermal degradation behavior of bacterial cellulose, Biomacrom 5 (5) (2004) 1671−1677.

[55] C.J. Garvey, I.H. Parker, G.P. Simon, On the interpretation of X-ray diffraction powder patterns in terms of the nanostructure of cellulose I fibres, Macrom. Chem. Phys. 206 (15) (2005) 1568−1575.

[56] F. Niu, M. Li, Q. Huang, X. Zhan, W. Pan, J. Yang, J. Li, The characteristic and dispersion stability of nanocellulose produced by mixed acid hydrolysis and ultrasonic assistance, Carbohydr. Polym. 165 (2017) 197−204.

[57] D.L. Dorset, Crystallography of the Polymethylene Chain: an Inquiry into the Structure of Waxes, Oxford Science University Ed., 2005, pp. 171−184.

[58] T. Theivasanthi, F.A. Christma, A.J. Toyin, S.C. Gopinath, R. Ravichandran, Synthesis and characterization of cotton fiber-based nanocellulose, Int. J. Biol. Macromol. 109 (2018) 832−836.

https://doi.org/10.1016/j.heliyon.2019.e01313